Materials Characterization 123 (2017) 264–274

Contents lists available at ScienceDirect

Materials Characterization

journal homepage: www.elsevier.com/locate/matchar

Phase structures and morphologies of tempered CA6NM stainless steel welded by hybrid laser-arc process

F. Mirakhorli [a,b,*], X. Cao [b], X-T. Pham [a], P. Wanjara [b], J.L. Fihey [a]

[a] École de Technologie Supérieure, Montréal, Québec H3C 1K3, Canada
[b] National Research Council Canada – Aerospace, Montréal, Québec H3T 2B2, Canada

ARTICLE INFO

Article history:
Received 10 June 2016
Received in revised form 19 October 2016
Accepted 27 October 2016
Available online 29 October 2016

Keywords:
Martensitic stainless steel
Welding
Post-weld heat treatment
Tempering
Microstructure
EBSD

ABSTRACT

The post-weld tempered microstructure of hybrid laser-arc welded CA6NM, a cast low carbon martensitic stainless steel, was investigated. The microstructural evolutions from the fusion zone to the base metal were characterized in detail using optical microscopy, scanning electron microscopy (SEM), electron backscatter diffraction (EBSD), X-ray diffraction (XRD) and microhardness techniques. The fusion zone, in its post-weld tempered condition, consisted of tempered lath martensite, residual delta-ferrite with various morphologies, reversed austenite and chromium carbides. The reversed austenite, which can be detected through both EBSD and XRD techniques, was found to be finely dispersed along the martensite lath boundaries, particularly at triple junctions. Based on the EBSD analysis, the orientation relationship between the reversed austenite and the adjacent martensite laths seemed to follow the Kurdjumov-Sachs (K-S) model. The results also revealed the presence of the reversed austenite in the different regions of the heat affected zone after post-weld tempering. The microindentation hardness distribution was measured, and correlated to the evolution of the corresponding microstructure across the welds.

Crown Copyright © 2016 Published by Elsevier Inc. All rights reserved.

1. Introduction

Cast CA6NM is a low carbon 13%Cr-4%Ni martensitic stainless steel (SS), which is widely used in hydroelectric turbine runners, pump castings and ship propellers. This alloy displays several important characteristics, including improved weldability, strength and corrosion resistance compared to typical martensitic SS, such as 410 SS. The mechanical properties, such as tensile strength, elongation and impact energy values, are all strongly dependent on the low carbon lath martensite (α') microstructure and the presence of other phases such as delta ferrite (δ), austenite (γ) and chromium carbides [1,2]. A three-level hierarchical organization of the lath α' structure has been proposed [3–5]. At the top of this hierarchy, the original γ grains are divided into a few packets, constituting an aggregation of blocks that are, in turn, composed of α' laths, as depicted in Fig. 1.

When a conventional multi-pass arc welding process is used for the assembly of thick components in CA6NM, both a large fusion zone (FZ) and heat-affected zone (HAZ) are usually generated. By contrast, the hybrid laser-arc welding (HLAW) process combines the high energy density laser source with the gas metal arc welding (GMAW) process that leads to a significant reduction in the size of the FZ and HAZ. Moreover, this combination of heating sources decreases the total heat input, while maintaining high productivity [6]. Several studies have been conducted to investigate the as-welded microstructure in both the FZ and HAZ of similar materials assembled using fusion welding processes. For example, Carrouge [7] and Enerhaug et al. [8] identified four different HAZs in the weldments of super martensitic SS using arc welding process. The same nomenclatures have also been used to describe the various HAZs in low carbon martensitic SS welds assembled with GMAW [9], and recently electron beam welding [10]. The effect of the HLAW process on the microstructure and the associated mechanical properties were also investigated for 10-mm-thick CA6NM plates welded with 410NiMo filler metal [11]. In these reported work, the evolution in the microstructural constituents in the FZ and HAZ have been postulated based on the Fe-Cr-Ni equilibrium phase diagram and characterized through optical microscopy (OM) and X-ray diffraction (XRD) analysis; but the nature of the phases was not discerned in detail, inevitably due to their inherently small size. In particular, conventional OM possesses restricted resolution and magnification, and phase detection/identification using XRD can be limited for very low volume fractions [12], depending on the incoming beam intensity and scanning speed, especially for textured polycrystalline samples. By contrast, electron backscatter diffraction (EBSD) with a field emission-scanning

* Corresponding author at: École de Technologie Supérieure, Montréal, Québec H3C 1K3, Canada.
E-mail addresses: Fatemeh.mirakhorli.1@ens.etsmtl.ca (F. Mirakhorli), Xinjin.cao@cnrc-nrc.gc.ca (X. Cao), Tan.pham@etsmtl.ca (X.-T. Pham), Priti.wanjara@cnrc-nrc.gc.ca (P. Wanjara), jean-luc.fihey@etsmtl.ca (J.L. Fihey).

http://dx.doi.org/10.1016/j.matchar.2016.10.029
1044-5803/Crown Copyright © 2016 Published by Elsevier Inc. All rights reserved.

Nomenclature

δ	delta-ferrite
γ	austenite
α′	martensite
Ac_1	temperature at which austenite begins to form during heating
Ac_3	temperature at which transformation of ferrite to austenite is completed during heating
Ac_4	temperature at which austenite transforms to delta ferrite during heating
Ac_5	temperature at which transformation of austenite to delta ferrite is completed during heating
bcc	body centered cubic
BM	base metal
EBSD	electron backscatter diffraction
fcc	face centered cubic
FE-SEM	field emission-scanning electron microscopy
FZ	fusion zone
GMAW	gas metal arc welding
HAZ	heat-affected zone
HLAW	hybrid laser-arc welding
IPF	inverse pole figure
IQ	image quality
K-S	Kurdjumov–Sachs
MUD	maximal multiple of uniform distribution
ND	normal direction
OM	optical microscopy
OR	orientation relationship
PAGB	prior-γ grain boundary
PF	pole figure
SEM	scanning electron microscopy
SS	stainless steel
TEM	transmission electron microscopy
TD	transverse direction
WD	welding direction
XRD	X-ray diffraction

electron microscope (FE-SEM) can provide quantitative microstructural information about the grain boundary orientation and characteristics, texture, crystallographic structure and phase identification using Kikuchi-pattern diffraction [13,14]. Furthermore, the combination of EBSD and FE-SEM enable the study of large areas (as compared to transmission electron microscopy (TEM)) with high accuracy and rapid speed.

Recently, Amrei et al. [15] used the EBSD method to characterize the complex microstructure and crystallographic textures in a multi-pass

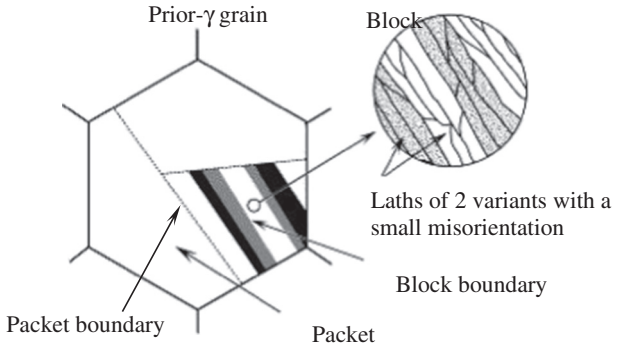

Fig. 1. Schematic illustration showing lath α′ structure in low carbon steels [5].

CA6NM weld manufactured using flux core arc welding. For hybrid laser-arc welded CA6NM, however, the main phases, morphologies, and crystallographic textures have not been reported, although these can influence the mechanical performance of the assembly [16]. In the present work, 10-mm-thick CA6NM plates were welded using a single-pass HLAW process. The microstructural evolution in both the FZ and HAZ was investigated in the post-weld tempered condition. Phase analyses were systematically performed using OM, XRD and EBSD-SEM techniques. The morphologies and crystallography of the different phases were studied in detail and correlated to the microindentation hardness profiles.

2. Material and Experimental Procedures

The CA6NM base metal (BM) plates used in this study were 10 mm thick, 150 mm long and 75 mm wide. The chemical composition is listed in Table 1. The plates were sectioned from a cast turbine runner blade that had been heat-treated according to the following procedures: (1) normalizing by first heating at a rate of 60 °C/h to 800 °C and holding for 8 h, followed by heating at a rate of 25 °C/h to 1030 °C and holding for 27 h, (2) air cooling below the α′ finish temperature (M_f) of 90 °C, and (3) tempering by heating at a rate of 36 °C/h to 640 °C and holding for 27 h, followed by cooling at a rate of 25 °C/h to room temperature. It is worth mentioning that the tempering temperature exceeded the maximum temperature of 620 °C specified by ASTM743 for CA6NM and that according to Thibault et al. [17] a tempering temperature above 630 °C would result in the transformation of some of the reversed γ into untempered α′ upon cooling.

The laser welding equipment consisted of an IPG Photonics 5.2 kW continuous wave solid-state Yb-fiber laser attached to an ABB robotic mounting arm. A collimation lens of 200 mm, a focal lens of 300 mm and a fiber diameter of 0.2 mm were employed to produce a nominal focusing spot diameter of ~0.30 mm. The defocusing distance was 2.5 mm beneath the top surface of the workpiece and the laser head was inclined 5° from the vertical position during welding. A Fronius Trans Pulse Synergic 4000 CMT (Cold Metal Transfer) GMAW power supply was used in combination with this laser system. The top surface of the workpiece was shielded using a mixture of 96% argon and 4% oxygen at a flow rate of 23.6 L/min that was fed through a GMAW nozzle, while the bottom surface was shielded using 100% argon at a flow rate of 9.5 L/min.

A single-pass HLAW process was developed to obtain full penetration for the 10-mm thick CA6NM plate using a Y-groove joint configuration. The bevel angle was ~30°. The root size was 5 mm with a gap size of ~0.2 mm. The chemical composition of the ER410NiMo filler wire (ϕ 1.14 mm) used in this process is provided in Table 1. HLAW trials were conducted at a laser power of 5.2 kW in "laser leading" mode with a welding speed of 1.0 m/min and a wire feed rate of 16 m/min. The arc current and voltage were 352 A and 30 V, respectively. Post-weld tempering was performed at a holding temperature of 600 °C for 1 h with heating and cooling rates of 50 °C/h.

After HLAW, metallographic specimens were extracted from the steady state region of the weld. Preparation for metallographic examination using OM and XRD involved (1) hot mounting of the specimens, (2) grinding with successively finer SiC papers from 240 to 1200 grit and (3) polishing with 3, 1 and 0.5 μm diamond suspensions. For EBSD analysis, the specimen extracted from the weld was machined to have two parallel surfaces prior to metallographic preparation, as described above. Subsequently, the EBSD specimen was vibrometry-polished for 20 h using a 0.05 μm colloidal silica suspension, followed by electro-polishing in a solution of 65 ml $HClO_4$, 550 mL ethanol, 70 mL butyl-cellosolve, and 70 mL H_2O at 25 °C and 25 V for 15 s.

For OM imaging, the specimens were etched chemically in Beraha's reagent (1 g K2S2O5 + 20 mL HCl + 80 mL H_2O) to reveal the α′ and δ in the microstructure. Alternatively, electro-etching in a 20% aqueous solution of NaOH at room temperature was used to reveal only the

Download English Version:

https://daneshyari.com/en/article/5454964

Download Persian Version:

https://daneshyari.com/article/5454964

Daneshyari.com